2024 IEEE 20th International Conference on Automation Science and Engineering (CASE)
August 28 - September 1, 2024. Bari, Italy

2024 IEEE 20th International Conference on Automation Science and Engineering (CASE) | 979-8-3503-5851-3/24/$31.00 ©2024 IEEE | DOI: 10.1109/CASE59546.2024.10711527

Long-term Water Quality Prediction based on Intelligent Optimization and Seasonal-trend Decomposition

Ziqi Wang[1], Xiangxi Wu[1], Jing Bi[1], Haitao Yuan[2], Jia Zhang[3] and MengChu Zhou[4]

***Abstract*—Nowadays, the applications of water quality prediction in the field of regional water environment management are increasing. It refers to predicting the elemental values of the water environment in the future based on past monitoring data, which is essential to realize the real-time evaluation of water quality and dynamic control of pollution sources. However, the water environment indicators are affected by various elements, which have a large volatility and non-linear characteristics. In addition, most of the existing water quality predictions focus on single-step predictive modeling of single elements of the water environment and lack multi-step predictive analysis of multi-factor data of the water environment. In this paper, a novel long-term prediction model based on genetic simulated annealing-based particle swarm optimization (GSPSO) with seasonal-trend decomposition using LOESS (STL) is proposed and named GSPSO-STL-Autoformer (GS-Autoformer). It realizes the multi-factor and long-term prediction of water quality time series data. Firstly, the Autoformer's hyperparameters are optimized by the GSPSO to improve its convergence speed. Secondly, the multi-factor features are decomposed by the STL to make the model more focused on learning feature information of each component. Finally, the long-term prediction is realized by the Autoformer. Comparative experiments with state-of-the-art peers show that the GS-Autoformer can effectively improve the accuracy of multi-factor and long-term predictions.**

***Index Terms*—Time series forecasting, seasonal-trend decomposition, intelligent optimization algorithms.**

I. INTRODUCTION

In recent years, the use of water quality prediction technology [1]–[3] has significantly increased in regional water environment management [4]–[6]. It predicts future elemental values of the water environment using past monitoring data [7], which is significant for real-time water quality assessment. However, the existing water quality prediction models still face some problems due to the great volatility and nonlinearity [8] of the changes in water quality indices. To be specific, the water environment multi-factor data is dynamically changed over time without specific regularity and stability. Since traditional machine learning [9] models, *e.g.*, autoregressive integrated moving average model cannot effectively reflect the non-linear distribution of short-term, high-frequency, and multi-factor data. In this case, there is still a lack of comprehensive methodological research on the change of short-term, high-frequency, and multi-factor indicators of the water environment. Furthermore, it is essential to extend the prediction time frame in practical applications [10]. Traditional end-to-end models [11] for dealing with sequence problems compress the data information when encoding long sequence data. However, with the emergence of long sequences, the loss of sequence information by encoding becomes gradually larger. Therefore, strong prediction ability and high computational efficiency of the model are required for realizing long-term water quality prediction.

Deep learning water quality prediction models and models based on multiple attention mechanisms provide solutions to the above problems. For instance, the long-short term memory model (LSTM) [12] can be adopted to efficiently extract water quality information based on periodic and non-linear changes [13]. Moreover, the Autoformer [14] can be applied in long-term temporal prediction, which is capable of predicting a longer-term future based on valid information. However, there are still three issues that require attention. The first problem is that traditional water quality prediction methods are not comprehensive enough to realize real-time prediction of multi-factor data [15]. Secondly, most of the existing water quality predictions focus on predictive modeling of a single element of the water environment and lack predictive analysis of multi-factor data. Finally, due to the stringent time requirements for water quality predictions, most existing works focus on analyzing the single-step prediction effect of single-element water quality. They do not consider the construction of multi-step and long-term prediction models for multi-factor data. Therefore, how to effectively utilize water quality time series data to achieve real-time, multi-step, and long-term prediction of multi-factor data on water quality is imperative.

Motivated by the aforementioned analysis, this work designs a multi-factor and long-term prediction model based on genetic simulated annealing-based particle swarm optimization (GSPSO) [16] and seasonal-trend decomposition using LOESS (STL) [17]. GSPSO is first adopted to optimize the hyperparameters of the prediction model. It reduces the process of manual parameter setting and avoids parameter setting deviation on prediction accuracy, which can also improve the

This work was supported by the National Natural Science Foundation of China under Grants 62173013 and 62073005, and the Beijing Natural Science Foundation under Grants L233005 and 4232049.

[1]Z. Wang, X. Wu and J. Bi are with the Faculty of Information Technology, Beijing Laboratory of Smart Environmental Protection, Beijing University of Technology, Beijing 100124, China. ziqi_wang@emails.bjut.edu.cn

[2]H. Yuan is with the School of Automation Science and Electrical Engineering, Beihang University, Beijing 100191, China. yuan@buaa.edu.cn

[3]J. Zhang is with the Department of Computer Science in the Lyle School of Engineering at Southern Methodist University, Dallas, TX 75205, USA. jiazhang@smu.edu

[4]M. Zhou is with the Department of Electrical and Computer Engineering, New Jersey Institute of Technology, Newark, NJ 07102 USA. zhou@njit.edu

convergence speed of the prediction model. Then, the STL is adopted to learn the periodicity and volatility characteristics among the long-term water quality data. Finally, the long-term prediction model is constructed and named GSPSO-STL-Autoformer (GS-Autoformer). Moreover, Autoformer reduces the complexity of the long-term prediction through an autocorrelation attention mechanism with a multi-head structure. Finally, the GS-Autoformer realizes efficient and accurate water quality prediction over a long period.

II. PROPOSED FRAMEWORK

A. Genetic Simulated annealing-based Particle Swarm Optimization

The multi-factor and long-term prediction model requires optimization of several hyperparameters, *e.g.*, the number of hidden layers, input length, and dropout rate. To avoid the impact of manually setting parameters on the prediction accuracy, an optimization algorithm named GSPSO is employed to choose the model's hyperparameters.

GSPSO integrates genetic learning and simulated annealing (SA) [18] into particle swarm optimization (PSO) [19] to balance its exploration and exploitation ability. In GSPSO, each particle is guided under its historical and the global best particle to update its position and velocity. It is assumed that the velocity of particle i is denoted as $V_i=(\nu_{i,1},\nu_{i,2},....,\nu_{i,D})$, where D represents the dimension of each particle. The position of particle i is denoted as $L_i=(l_{i,1},l_{i,2},....,l_{i,D})$. $P_i=(p_{i,1},p_{i,2},....,p_{i,D})$ denotes the historical optimum of particle i and $G=(g_1,g_2,....,g_D)$ denotes the global optimum of the population. In addition, $v_{i,d}$ and $l_{i,d}$ are velocity and position of dimension d for particle i, respectively. Specifically, they are updated as:

$$\nu_{i.d}=\hat{b}.\nu_{i.d}+c_1\cdot r_{1.d}\cdot(p_{i.d}-l_{i.d})+c_2\cdot r_{2.d}\cdot(g_d-l_{i.d}) \quad (1)$$

$$l_{i,d}=l_{i,d}+v_{i,d} \quad (2)$$

$$\hat{b}=b_{\max}-\frac{b_{\max}-b_{\min}}{a_{\max}}a \quad (3)$$

where $\hat{b}$ denotes the inertia weight. The acceleration coefficients c_1 and c_2 establish the relative importance of P_i and G, respectively. $r_{1,d}$ and $r_{2,d}$ are random values in [0,1]. b_{max} and b_{min} are the maximum and minimum values of $\hat{b}$. a and a_{max} denote the current and maximum number of iterations.

Particle i of the population learns from its historical optimum P_i and the global optimum G. However, if both converge to the same local optimum, the algorithm may cease exploring further, leading to premature convergence. As a result, for each particle i, a combination sample $E_i=(e_{i,1},e_{i,2},....,e_{i,D})$ is formulated to guide its searching direction. Moreover, E_i enhances the diversity of the population and thus helps the algorithm to move out of local optima. $e_{i,d}$ is adopted to vary the velocity of each particle and it is updated with (4) and (5).

$$\nu_{i.d}=\hat{b}.\nu_{i.d}+c\cdot r_d\cdot(e_{i.d}-l_{i.d}) \quad (4)$$

$$e_{i,d}=\frac{c_1\cdot r_{1,d}\cdot p_{i,d}+c_2\cdot r_{2,d}\cdot g_d}{c_1\cdot r_{1,d}+c_2\cdot r_{2,d}} \quad (5)$$

where c is a coefficient and r_d is a random value in [0,1].

B. Seasonal-trend Decomposition using LOESS (STL)

STL is adopted for decomposing time series into three components including trend terms, seasonal terms, and residual terms. STL contains a series of locally weighted regression smoother and uses Loess to extract the smoothing estimates of the three components, where Loess is a method for estimating non-linear relationships. The formula for decomposing time series data is shown in (6).

$$Y_v=T_v+S_v+R_v \quad (6)$$

where Y_v denotes the original time series at time v. T_v denotes the trend component at time v, which represents the low-frequency and long-time variation of the time series data. S_v is the seasonal component at time v, which represents the periodic change of time series data and R_v is the residual component at time v, which represents the residual value after removing the above two components. The architecture of the STL consists of an inner and outer loop, where the seasonal and trend terms are updated with each iteration of the inner loop. Each iteration of the outer loop includes the inner loop and the computation of the robustness weights, which is used to minimize the effect of temporary, outlying points on the trend and seasonal terms.

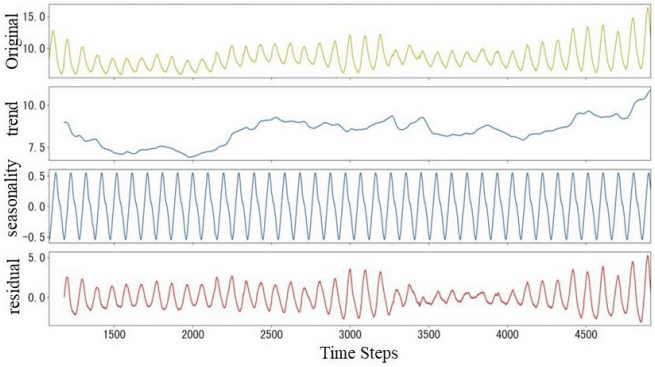

Fig. 1. Decomposition of the DO index by STL.

In this work, STL is first utilized to decompose the predicted DISSOLVED OXYGEN (DO) into three subsequences, including trend terms, seasonal terms, and residual terms. Then, the three sub-sequences are input to the model along with other elements in the dataset as feature dimensions. It enables the model to concentrate more on learning the complex features of the data, thus enhancing prediction accuracy. Fig. 1 illustrates the data distribution of STL's decomposition of the sequence DO.

C. Overall Architecture of the GS-Autoformer

Fig. 2 illustrates the overall structure of the GS-Autoformer. It is assumed that $X_i=(x_1,x_2,....,x_t)$ represents the value of water quality indicators at different time

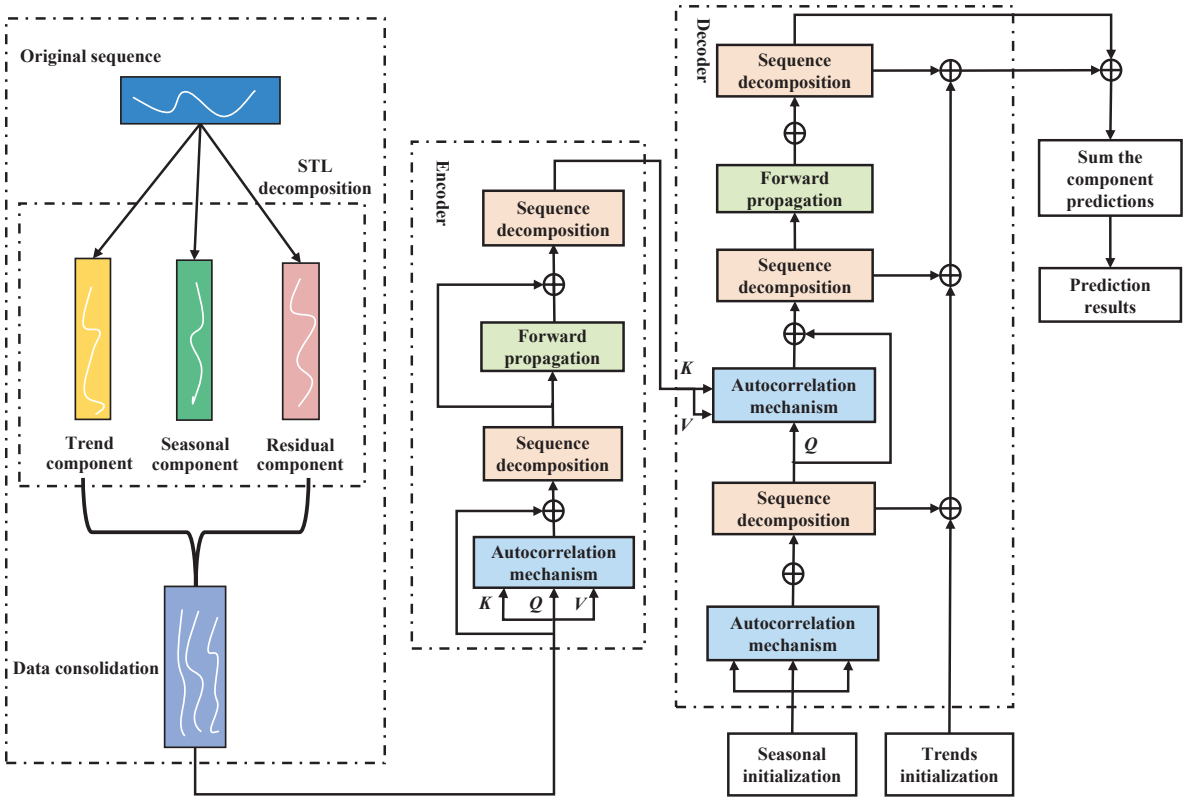

Fig. 2. Structure of GS-Autoformer.

points in the past. Firstly, the features to be predicted in the water quality indicators are decomposed by the STL into three components including trend, season, and residual. Then, these three components are merged with other features in the original series and then input to the Autoformer. The decomposition process of the STL is shown in (7).

$$\overline{X} = \mathbf{STL}(X, s) \tag{7}$$

where $\mathbf{STL}(\cdot)$ denotes the decomposition process using STL. $\overline{X}$ denotes the sequence that is input to the encoder and s denotes the timing cycle.

The Autoformer has an encoder-decoder structure [20], where the encoder and decoder simultaneously consist of three modules per layer, namely autocorrelation mechanism, sequence decomposition, and forward propagation. The encoder receives the STL decomposed data as input and focuses on the seasonal trend. Then, the past seasonal information is output to the decoder which helps it to adjust the prediction results. The decoder adopts an autocorrelation mechanism to model seasonal terms and predict their trend separately. The autocorrelation mechanism incorporates a multi-head attention mechanism, and its structure is shown in Fig. 3. For the trend term, the cumulative method extracts the trend information from the predicted hidden variables. Finally, the prediction results of the above components are added together to obtain the final prediction result.

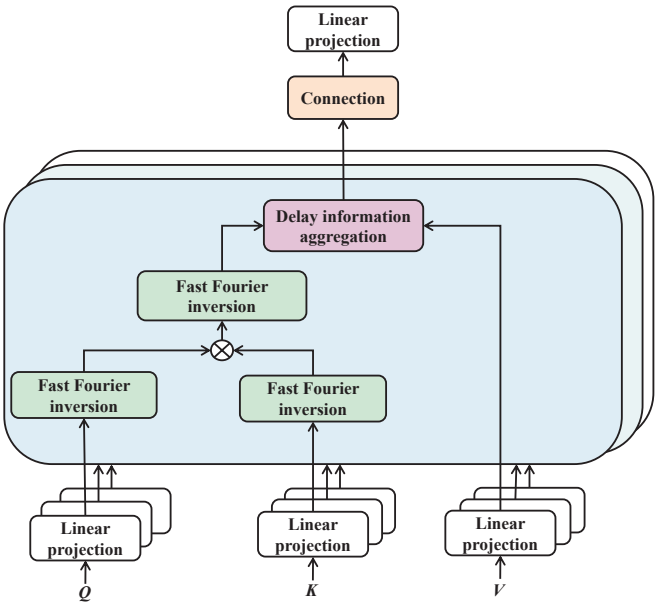

Fig. 3. Autocorrelation mechanism.

III. Experimental Results and Discussion

A. Selection and Processing of Datasets

This paper adopts the dataset from the Wucun automatic station in Langfang City released by the National Real-time

Data Distribution System of China [21]. The first field of each data point indicates the monitoring time, and the other fields indicate the monitoring values of the corresponding water quality element. Moreover, the time series data need to be converted into supervised data by using a sliding window [22] according to the input step of the prediction model. Therefore, the GS-Autoformer can make a single or multi-step prediction of the data indexes, and the specific process of the data transformation is shown in Fig. 4. Then, the data are divided into training, validation, and test sets under 7:1:2.

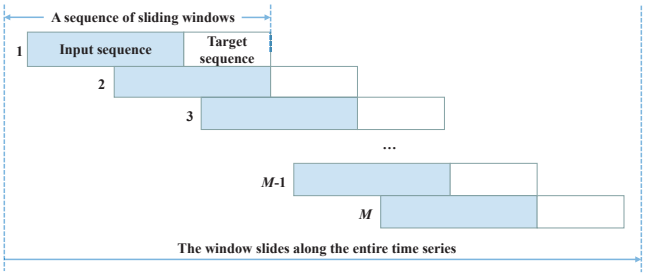

Fig. 4. Time-series data to supervised data.

B. Experimental Results

GS-Autoformer is compared with Transformer [23] and Informer [24] under the prediction step size of (12, 18, 24, 30, 48). Moreover, the optimal parameter setting of each model is determined by experiments. Finally, the prediction accuracy of each model is compared.

1) Transformer: The Transformer is adopted to realize the long-term prediction. During the model's training process, optimal prediction performance is achieved by adjusting two parameter sets: the lengths of the encoder/decoder inputs and the number of encoder/decoder layers.

Table I demonstrates the parameters adjustment process of the Transformer with a prediction step length of 12 as an example, where α and β denote the input length of the encoder and decoder, respectively. η and θ denote the encoder and decoder layers, respectively. It is shown that the optimal value setting of the input length is 24 and that of the decoder length is 12. Moreover, the optimal value settings of the encoder and decoder layers are both 1. Fig. 5 shows the predictive effect of the model after selecting the optimal parameters. It shows the fitting curve of the Transformer in predicting the DO metrics at 12 steps, where the blue curve denotes the true value and the red curve denotes the prediction value.

Table II shows the RMSE, MAE, and MAPE values for the Transformer with prediction steps (12, 18, 24, 30, 48). During the training process, the parameters of α, β, η, and θ are set as the previous experimental values. Moreover, the number of multi-attention mechanism headers is set to 8. The dimension of the model is 512 and the dropout is set to 0.05, which aims to prevent the overfitting problems of the model.

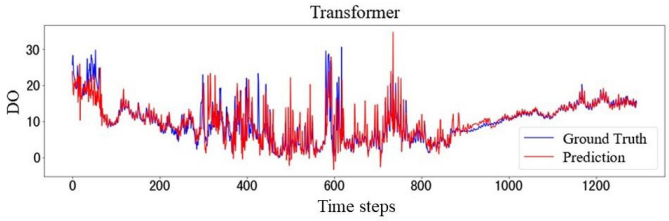

Fig. 5. Fitting diagram of Transformer in 12-step prediction.

TABLE I
RMSE FOR DIFFERENT ENCODER/DECODER INPUT LENGTHS AND LAYERS IN TRANSFORMER

Input Lengths: (α, β)	RMSE
(12, 6)	0.769
(24, 12)	**0.751**
(24, 6)	0.775
(32, 12)	0.857
(48, 32)	0.803
(48, 24)	0.768
(48, 6)	0.809

layers: (η, θ)	RMSE
(1, 1)	**0.747**
(1, 2)	0.834
(2, 1)	0.751
(2, 2)	0.761

TABLE II
PREDICTION RESULTS OF TRANSFORMER UNDER DIFFERENT PREDICTION STEPS

Predicted step size	Transformer		
	RMSE	MAE	MAPE
12	0.751	0.533	2.379
18	0.804	0.596	2.600
24	0.830	0.639	2.880
30	0.976	0.730	3.456
48	0.941	0.685	2.917

2) Informer: Informer is widely applied in the long-term prediction of multi-factor data. The same parameters adjustment process is applied for the Informer. The final parameters are set as follows: the encoder input length is 32, the decoder input length is 12, and the number of encoder and decoder layers are 2 and 1, respectively. The number of heads of the multi-head attention mechanism is set to 8, the dimension of the model is 512, and the value of the dropout is set to 0.05.

Fig. 6 demonstrates the predictive effect of the model after selecting the optimal parameters. It shows the fitting curve of the Informer in predicting the DO metrics at 12 steps. Moreover, it is shown that the predicted value has some deviation from the true value. Table III demonstrates the prediction effect of Informer with prediction steps of (12, 18, 24, 30, 48). The prediction results are evaluated by RMSE, MAE, and MAPE.

3) GS-Autoformer: The proposed GS-Autoformer is utilized to achieve long-term prediction of multi-factor data. Firstly, GSPSO optimizes Autoformer's hyperparameters, including the encoder input length, the decoder input length, and the dropout. The RMSE of the Autoformer with different combinations of the hyperparameters are shown in Table IV. It is shown that the GSPSO finds the optimal prediction effect

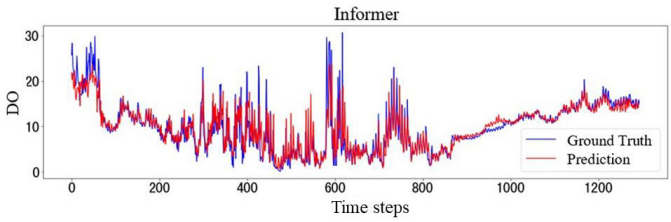

Fig. 6. Fitting diagram of Informer in 12-step prediction.

TABLE III
PREDICTION RESULTS OF INFORMER UNDER DIFFERENT PREDICTION STEPS

Predicted step size	Informer		
	RMSE	MAE	MAPE
12	0.797	0.610	2.944
18	0.880	0.671	2.990
24	0.798	0.612	2.732
30	1.067	0.855	3.131
48	0.965	0.774	3.168

of the model when the encoder input length is 30, the decoder input length is 24, and the dropout is 0.1. Moreover, Fig. 7 shows the fitting results of the GS-Autoformer in predicting the DO indicator at 12 steps, where the blue curve denotes the true values (Ground Truth), and the red curve denotes the predictions (Prediction). It is shown that the prediction curve well fits the true value curve.

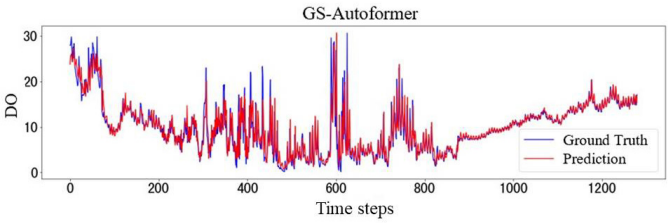

Fig. 7. Fitting diagram of GS-Autoformer in 12-step prediction.

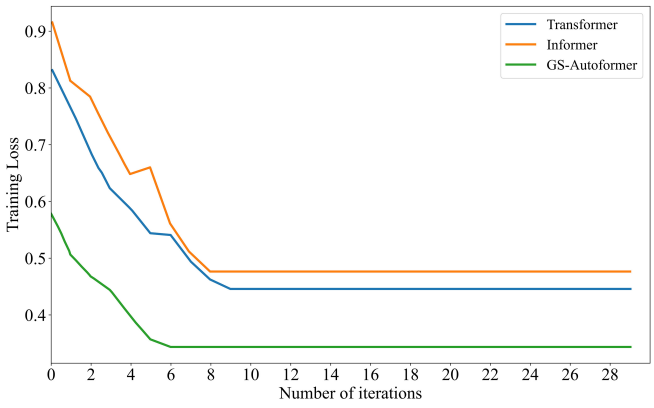

Fig. 8. Training loss of different models in 12-step prediction.

TABLE IV
RMSE OF AUTOFORMER UNDER DIFFERENT COMBINATIONS OF HYPERPARAMETERS

Group	Encoder length	Decoder length	Dropout	RMSE
1	24	24	0.1	0.779
2	30	24	0.7	0.814
3	30	12	0.1	0.780
4	24	12	0.1	0.795
5	30	12	0.7	1.116
6	24	12	0.7	0.867
GSPSO	**30**	**24**	**0.1**	**0.743**

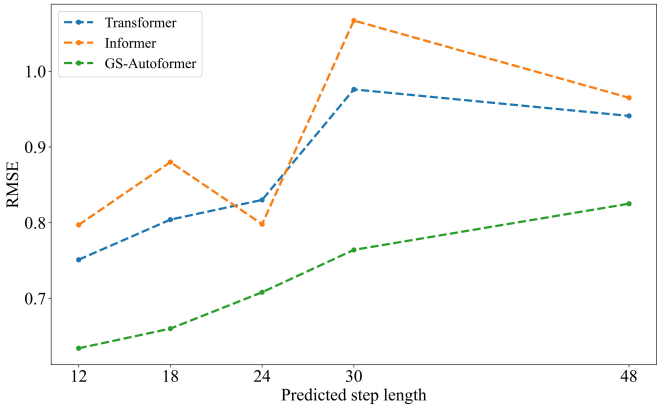

Fig. 9. RMSE of different models under different prediction steps.

Fig. 8 shows the variation of the training loss for the three models in predicting the DO metrics for 12 steps. It is shown that the Transformer has a training loss of 0.445 after 11 iterations, and the training loss of the Informer is 0.475 after 10 iterations. Moreover, GS-Autoformer has a training loss of 0.343 after 7 iterations. Therefore, the GS-Autoformer has faster training convergence speeds and small training loss, which outperforms the compared models. Furthermore, the RMSE of the Transformer, Informer, and GS-Autoformer for different predicted step lengths are shown in Fig. 9. It is shown that the GS-Autoformer has the smallest RMSE values among all different predicted step lengths, which proves its superiority in multi-factor and long-term prediction. The better prediction performance of the GS-Autoformer is firstly due to the GSPSO in the model. It adjusts the hyperparameters of the Autoformer, which avoids the influence of manual parameter adjustment. Moreover, the STL decomposition is adopted and coordinated with the Autoformer. Therefore, it can better learn the features of each component decomposed by the STL, which has advantages in improving the prediction accuracy. Finally, due to the decomposition architecture within the model and the autocorrelation mechanism, the prediction ability of the model is enhanced and the computational complexity of it is reduced, which ensures the robustness of the GS-Autoformer.

IV. CONCLUSIONS

Water quality prediction is an important task in pollution prevention of the water environment, which is significant in promoting the sustainable utilization of water resources. However, most of the existing water quality prediction methods focus on single-step predictive modeling of a single element, which lacks multi-element data and multi-step predictive analysis. This paper proposes a multi-factor and long-term prediction model for the water environment. It adopts genetic simulated annealing-based particle swarm optimization (GSPSO) to optimize the hyperparameters of the model and select the optimal parameter settings. Secondly, considering that the overall trend of the predicted data shows a certain seasonal regularity, the model adopts a seasonal-trend decomposition using LOESS (STL) to decompose the data features into trend terms, seasonal terms, and residual terms. It enables the model to learn the features of each component more attentively, thereby improving the prediction accuracy. Finally, GSPSO-STL-Autoformer (GS-Autoformer) is proposed to realize the multi-factor and long-term prediction. Moreover, GS-Autoformer internally reduces computational complexity and ensures the timeliness of the prediction through an autocorrelation mechanism. Finally, comparative experiments show that GS-Autoformer effectively improves the accuracy of multi-factor and long-term predictions.

In future work, we consider further incorporating the spatial dimension [25] into our model. To be specific, the spatial dependence information of each monitoring station is obtained to realize the spatio-temporal prediction of multi-factor data, which further enhances the application value of our GS-Autoformer.

REFERENCES

[1] L. Jia, N. Yen and Y. Pei, "Spatial and Temporal Water Quality Data Prediction of Transboundary Watershed Using Multiview Neural Network Coupling," *IEEE Transactions on Geoscience and Remote Sensing*, vol. 61, pp. 1–16, Nov. 2023.

[2] A. Biswas, Y. Lee and S. Manandhar, "Rainfall Forecasting Using GPS-Derived Atmospheric Gradient and Residual for Tropical Region," *IEEE Transactions on Geoscience and Remote Sensing*, vol. 60, pp. 1–10, Nov. 2022.

[3] Y. Wang, I. W. -H. Ho, Y. Chen, Y. Wang and Y. Lin, "Real-Time Water Quality Monitoring and Estimation in AIoT for Freshwater Biodiversity Conservation," *IEEE Internet of Things Journal*, vol. 9, no. 16, pp. 14366–14374, Aug. 2022.

[4] D. Xiang, X. Zhang, W. Wu and H. Liu, "DensePPMUNet-a: A Robust Deep Learning Network for Segmenting Water Bodies From Aerial Images," *IEEE Transactions on Geoscience and Remote Sensing*, vol. 61, pp. 1–11, Mar. 2023.

[5] H. Mohapatra, B. K. Mohanta, M. R. Nikoo, M. Daneshmand and A. H. Gandomi, "MCDM-Based Routing for IoT-Enabled Smart Water Distribution Network," *IEEE Internet of Things Journal*, vol. 10, no. 5, pp. 4271–4280, Mar. 2023.

[6] M. Singh, K. S. Sahoo and A. Nayyar, "Sustainable IoT Solution for Freshwater Aquaculture Management," *IEEE Sensors Journal*, vol. 22, no. 16, pp. 16563–16572, Aug. 2022.

[7] C. Li, L. Guo, H. Gao and Y. Li, "Similarity-Measured Isolation Forest: Anomaly Detection Method for Machine Monitoring Data," *IEEE Transactions on Instrumentation and Measurement*, vol. 70, pp. 1–12, Mar. 2021.

[8] T. Dimier and J. Biela, "Semi-Analytical Non-Linear Physical Model of Core Losses in Ferrite Ring Cores," *IEEE Transactions on Magnetics*, vol. 59, no. 11, pp. 1–5, Nov. 2023.

[9] Y. Shin and Y. Yoon, "Incorporating Dynamicity of Transportation Network With Multi-Weight Traffic Graph Convolutional Network for Traffic Forecasting," *IEEE Transactions on Intelligent Transportation Systems*, vol. 23, no. 3, pp. 2082–2092, Mar. 2022.

[10] Y. Ding, W. Lu, Y. Zhang, Y. Feng and Y. Zhou, "Study on the Practical Application of Surface Acoustic Wave Yarn Tension Sensor," *IEEE Transactions on Industrial Electronics*, vol. 69, no. 12, pp. 13781–13790, Dec. 2022.

[11] J. Wang, D. Gao and Q. Suolang, "Research on End-to-end Tibetan Speech Recognition Acoustic Model Based on Multi-scale Features," *2023 IEEE 4th International Conference on Pattern Recognition and Machine Learning (PRML)*, 2023, Urumqi, China, pp. 458–462.

[12] J. Bi, H. Yuan, K. Xu, H. Ma and M. Zhou, "Large-scale Network Traffic Prediction With LSTM and Temporal Convolutional Networks," *2022 International Conference on Robotics and Automation (ICRA)*, 2022, Philadelphia, USA, pp. 3865–3870.

[13] H. Bao, T. Zhang, D. Ding, R. Chen and D. H. Werner, "Generalized Periodic Boundary Conditions for DGTD Analysis of Arbitrary Skewed Periodic Structures," *IEEE Transactions on Microwave Theory and Techniques*, vol. 70, no. 6, pp. 2989–2998, Jun. 2022.

[14] W. V. Kambale, D. K. Kadurha, A. Deeb, F. A. Machot, T. Bernabia and K. Kyamakya, "Transformers in Time Series Forecasting: A brief Analysis of the Autoformer Transfer Learning Performance," *2023 30th IEEE International Conference on Electronics, Circuits and Systems (ICECS)*, 2023, Istanbul, Turkiye, pp. 1–6.

[15] J. Ling, Q. Chen, D. Liu, H. Sang, T. Wang and F. Shi, "Real-Time Desorption Flow Prediction of Automobile Carbon Canister for Virtual Calibration," *2022 IEEE 2nd International Conference on Electronic Technology, Communication and Information (ICETCI)*, 2022, Changchun, China, pp. 55–60.

[16] H. Yuan, Q. Hu, M. Wang, J. Bi and M. Zhou, "Cost-minimized User Association and Partial Offloading for Dependent Tasks in Hybrid Cloud–edge Systems," *2022 IEEE 18th International Conference on Automation Science and Engineering (CASE)*, 2022, Mexico City, Mexico, pp. 1059–1064.

[17] A. Krechiem and M. T. Khadir, "Algerian Electricity Consumption Forecasting with Artificial Neural Networks Using a Multiple Seasonal-Trend Decomposition Using LOESS," *2023 International Conference on Decision Aid Sciences and Applications (DASA)*, 2023, Annaba, Algeria, pp. 586–591.

[18] Y. Zhou, W. Xu, Z. -H. Fu and M. Zhou, "Multi-Neighborhood Simulated Annealing-Based Iterated Local Search for Colored Traveling Salesman Problems," *IEEE Transactions on Intelligent Transportation Systems*, vol. 23, no. 9, pp. 16072–16082, Sept. 2022.

[19] Z. Chen, K. Cao, R. Wu, L. Zhang, X. -D. Zhang and R. Chen, "Empirical Model and PSO-Based Algorithm for Efficient Measurement of Gas Permeation Through High Barrier," *IEEE Transactions on Instrumentation and Measurement*, vol. 71, pp. 1–8, Feb. 2022.

[20] K. Feng, H. Chen, Y. Kong, L. Zhang, X. Yu and W. Yi, "Prediction of Multi-Function Radar Signal Sequence Using Encoder-Decoder Structure," *2022 7th International Conference on Signal and Image Processing (ICSIP)*, 2022, Suzhou, China, pp. 1–6.

[21] J. Bi, L. Zhang, H. Yuan, J. Zhang, "Multi-indicator water quality prediction with attention-assisted bidirectional LSTM and encoder-decoder," *Information Sciences*, vol. 625, pp.65–80, May 2023.

[22] M. Lin, D. Wu, S. Chen, J. Meng, W. Wang and J. Wu, "Battery Health Prognosis Based on Sliding Window Sampling of Charging Curves and Independently Recurrent Neural Network," *IEEE Transactions on Instrumentation and Measurement*, vol. 73, pp. 1–9, Jan. 2024.

[23] X. Song, Z. Hua and J. Li, "Remote Sensing Image Change Detection Transformer Network Based on Dual-Feature Mixed Attention," *IEEE Transactions on Geoscience and Remote Sensing*, vol. 60, pp. 1–16, Sept. 2022.

[24] Y. Zhang, W. Zhou, J. Huang, X. Jin and G. Xiao, "Temporal Knowledge Graph Informer Network for Remaining Useful Life Prediction," *IEEE Transactions on Instrumentation and Measurement*, vol. 72, pp. 1–10, Sept. 2023.

[25] J. Kong, H. Deng and M. Jiang, "Symmetrical Enhanced Fusion Network for Skeleton-Based Action Recognition," *IEEE Transactions on Circuits and Systems for Video Technology*, vol. 31, no. 11, pp. 4394–4408, Nov. 2021.